Paleontological Research, vol. 6, no. 1, pp. 101–120, April 30, 2002

Taphonomy of the bivalve assemblages in the upper part of the Paleogene Ashiya Group, southwestern Japan

NORIHIKO SAKAKURA

Department of Geology and Mineralogy, Kyoto University, Kyoto 606-8502, Japan
(E-mail: sakakura@kueps.kyoto-u.ac.jp)
Present address: Research Institute for Integrated Science, Kanagawa University, 2946 Tsuchiya, Hiratsuka, 259-1205, Japan

Received 18 August 2000; Revised manuscript accepted 30 November 2001

Abstract. **The Paleogene Ashiya Group, in which molluscan fossils are abundant (= Ashiya fauna), consists mainly of shallow marine deposits that exhibit sedimentary cycles especially in the Waita Formation (upper part of the Group). Each cycle is redefined as a thin transgressive basal sandstone (transgressive systems tract) overlain by a progradational coarsening-upward interval (highstand systems tract). The depositional environment varies from a shallower condition influenced by strong wave action (shoreface?) to a deeper condition below the storm wave base, which is followed by next shallower conditions such as lower shoreface or intertidal zone. Molluscan fossils occur only from the thin lower part of each cycle, namely the transgressive basal sandstone and from the mudstone of the earliest progradational phase. The fossils occur both as shell concentrations and more dispersed fossiliferous deposits. Bed-by-bed sampling based on taphonomic, sedimentologic and paleoecologic observations distinguishes four fossil assemblages, (a) *Glycymeris-Phacosoma*, (b) *Venericardia-Crassatella*, (c) *Venericardia* and (d) *Yoldia-Nucula*. These assemblages occur successively in each cycle, and their taphonomic features also change upward from a wave-generated allochthonous shellbed on the basal ravinement surface to autochthonous shell patches. The successive change accompanies a decreasing wave-influence during a transgressive period. Epibionts, such as epifaunal byssally attached bivalves and barnacles, occur abundantly as associated species of the *Venericardia-Crassatella* assemblage from the middle part of the transgressive basal sandstone. Epibiontic colonization probably reflects taphonomic feedback, with shelly substrates avoiding burial by the winnowing of sediments during transgression. Autochthonous shellbeds dominated by *Venericardia subnipponica* are intercalated in the glauconitic sandstone beds (surface of maximum transgression) at the top of the transgressive basal sandstone. The shellbeds probably represent an attritional accumulation with dead shells of *Venericardia* supplied continuously *in situ* during a phase of low sediment supply.**

Key words: **Ashiya Group, bivalves, paleoecology, Paleogene, sedimentary cycle, transgression**

Introduction

The Ashiya Group is the uppermost sequence of coal-bearing Paleogene deposits in the northern limb of Kyushu. It consists of shallow marine sandstones and mudstones, and is biostratigraphically assigned to the latest Early Oligocene age by calcareous nannoplankton and foraminifera (Saito and Okada, 1984; Tsuchi *et al.*, 1987). It was lithostratigraphically subdivided into the Yamaga, Sakamizu, and Waita Formations in upward sequence (Nagao, 1927a, 1928a; Okabe and Ohara, 1972 etc.). Recently the stratigraphic division was revised by Ozaki *et al.* (1993), in which the Yamaga, Norimatsu, Jinnobaru, Honjo and Waita Formations were redefined. Hayasaka (1991) investigated the group sedimentologically, distinguished 23 coarsening-upward sedimentary cycles, and gave their environmental interpretations.

Abundant molluscan fossils from the Group are called the Ashiya Fauna and represent the typical molluscan fauna of Oligocene age in west Japan (Nagao, 1927a, 1928a; Otsuka, 1939; Oyama *et al.*, 1960 etc.). The molluscan fossils have been taxonomically and biostratigraphically studied by several authors (Nagao, 1927b, 1928b; Mizuno, 1963 etc.). In addition, the molluscan fauna from the Jinnobaru Formation was studied paleoecologically (Shuto and Shiraishi, 1971).

However, little is known about the precise relation between sedimentary cycles and the molluscan assemblages, which exhibit characteristic modes of occurrence by facies. Taphonomic features of the molluscan assemblages also re-

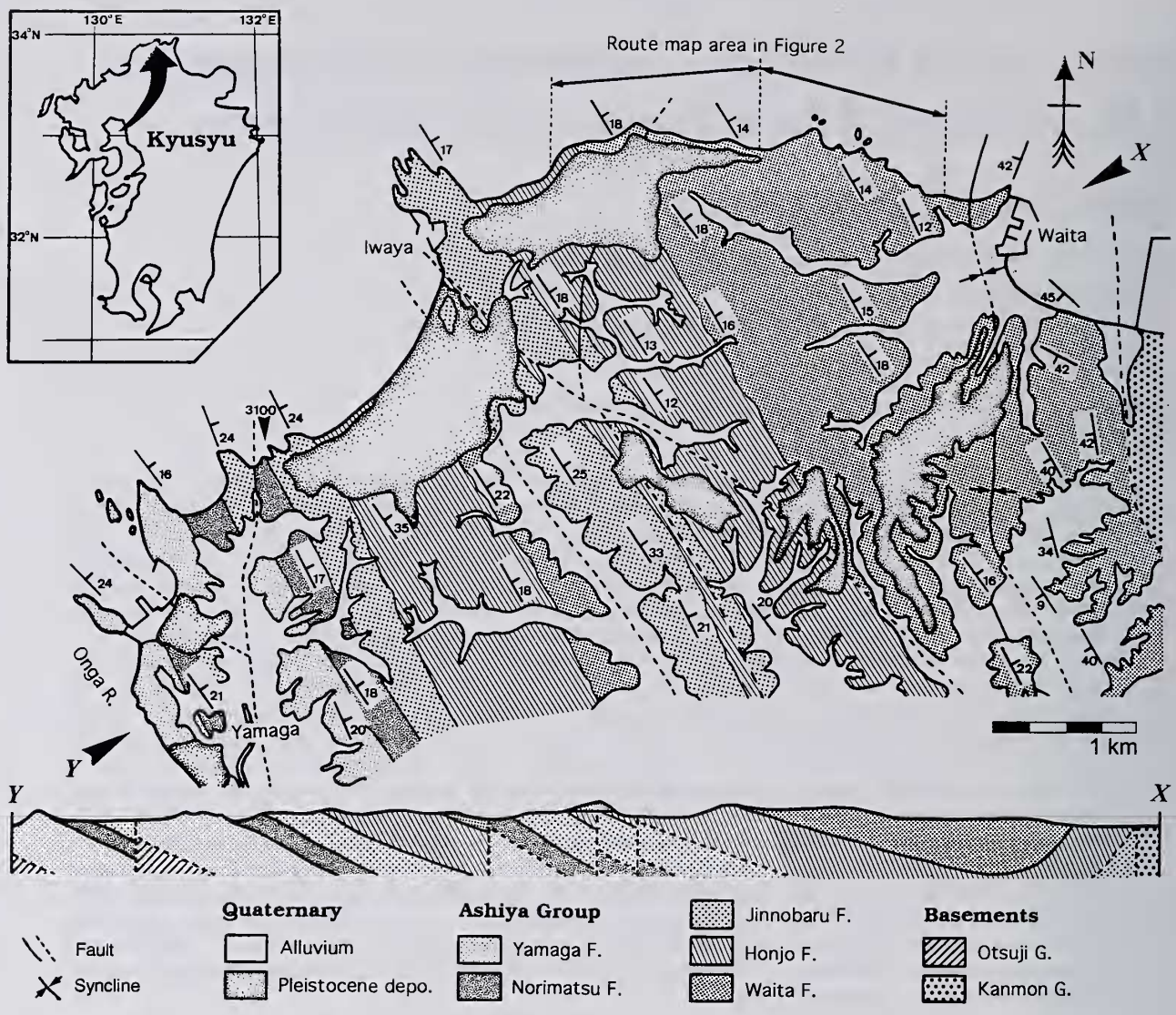

Figure 1. Geologic map of the Wakamatsu area, Kitakyushu, northern Kyushu. Route-mapped area in Figure 2 indicated by thick arrows and Locality 3100 are shown.

main largely to be investigated.

To clarify these problems, I closely examined the sedimentary features and modes of fossil occurrence of the Ashiya Group bed-by-bed. Through detailed observations, particularly in the Waita Formation (the upper part of the Group), I discovered a close relationship between the sedimentary cycle and the composition and mode of occurrence of bivalve assemblages. These changes are commonly repeated in every cycle of the Waita Formation.

This paper aims to reconstruct the sedimentological and paleoecological processes in the Ashiya Group based on detailed observations of its sedimentological and taphonomic features. My aims here are to: (1) redefine the sedimentary cycles in the Waita Formation and describe its lithofacies, (2) describe modes of occurrence and the succession of the molluscan assemblages in the cycle, and (3) discuss the formative process of the sedimentary and paleoecological succession.

Geological setting

The Ashiya Group in the study area is bounded on the east by a fault of NNW-SSE trend, and on the west by the Onga River. The strata of the group strike N 20–45° W and dip 10–30° gently northeastward except for those in the eastern limb of the syncline (Figure 1). In the eastern limb, the strata steeply strike N 10–50° W and dip 45° W. At least seven faults of similar NW-SE trend are observed

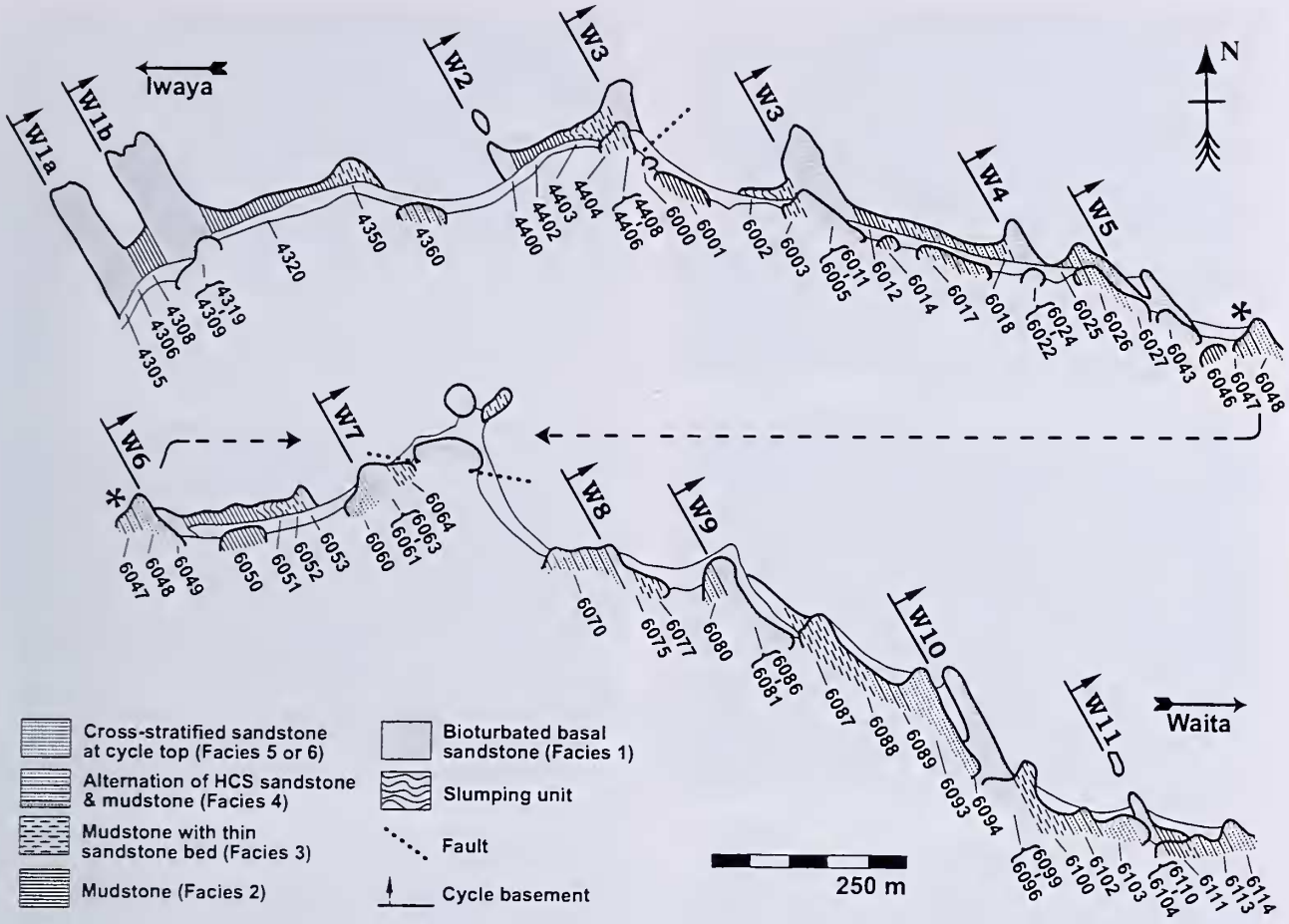

Figure 2. Route map from the Iwaya to Waita coast (Figure 1). The left section connected to the right at the asterisks (*). Localities and redefined sedimentary cycles are shown.

or estimated.

The Ashiya Group is subdivided into the Yamaga, Norimatsu, Jinnobaru, Honjo and Waita Formations in ascending order (Ozaki *et al.*, 1993). The lowermost Yamaga Formation is characterized by bioturbated fine sandstones. The formation is more than 170 m thick, although the basal part is unexposed. The succeeding Norimatsu Formation consists of the alternating sandstone and mudstone, and is 50–70 m thick. Both formations crop out in the western part of the study area (Figure 1).

The Jinnobaru Formation consists of sandstones in which hummocky cross-stratification is occasionally observed, and is 140–260 m thick. The Honjo Formation consists of sandstones and mudstones, exhibits sedimentary cycles, and is about 230 m thick. Both formations crop out in the central part of the area from north to south (Figure 1).

The Waita Formation (uppermost of the Group) exhibits clear sedimentary cycles composed of sandstones and mudstones (Figure 2). It is widely distributed in the eastern part of the area, and is more than 450 m thick, although the top part is unexposed (Figure 1).

Sedimentary cycles

The upper part of the Ashiya Group (Honjo and Waita Formations) consists of coarsening-upward sedimentary cycles (Hayasaka, 1991; Ozaki *et al.*, 1993). Each cycle is 30–100 m thick (Figure 3), and consists of various sandstones and mudstones. At least 11 sedimentary cycles, named W1–W11 in ascending order, are recognized in the Waita Formation (Hayasaka, 1991; Ozaki *et al.*, 1993). Previous studies defined the sedimentary cycles as coarsening-upward lithologic change, which begins with a mudstone interval and ends with a sandstone interval (Hayasaka, 1991, p. 617, fig. 5; Figure 3).

However, close examination indicates that the definition of the cycles must be revised. Specifically, there is a sharp erosional surface within the upper sandstone interval of

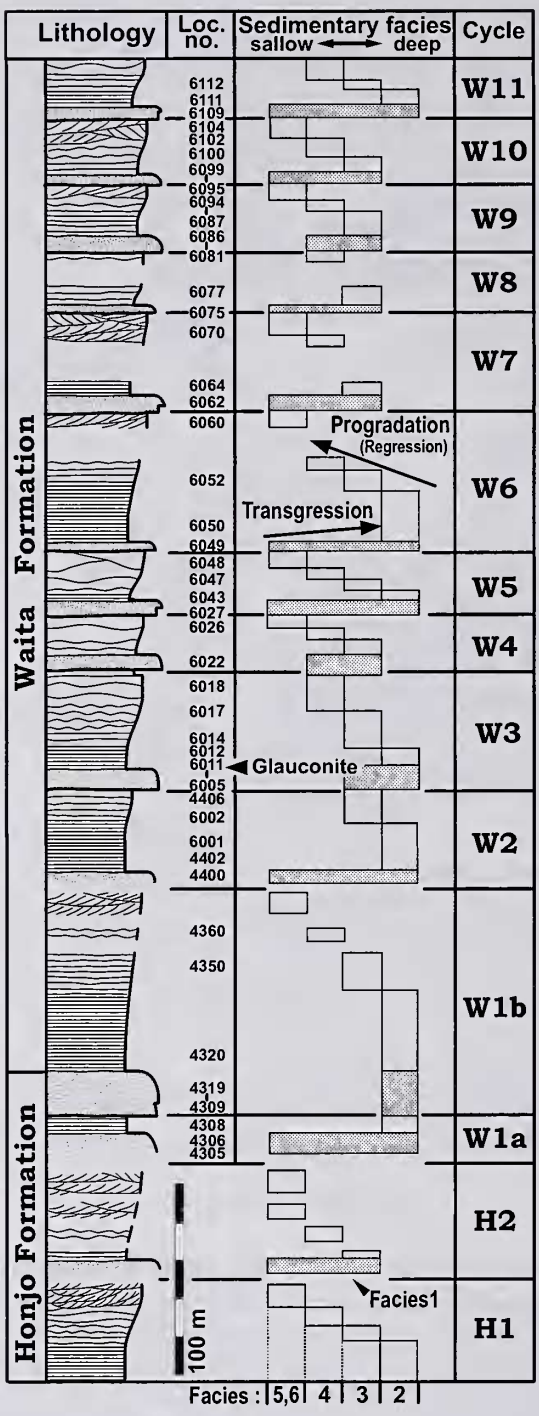

Figure 3. Columnar section of the Waita Formation exposed along the Iwaya to Waita coast. At least 11 sedimentary cycles, W1-W11 in ascending order, are recognized in the Waita Formation. Facies 1–6 indicate sedimentary facies in a cycle: transgressive basal sandstone (Facies 1), mudstone (Facies 2), mudstone interbedded with very thin sandstone beds (Facies 3), alternation of HCS sandstone and mudstone (Facies 4), amalgamated HCS sandstone (Facies 5), and tabular cross-stratified sandstone (Facies 6) in order. Glauconite sandstone bed is intercalated at the top of the transgressive basal sandstone of the Cycle 3. Facies 2–4 compose the progradational coarsening-upward interval.

each previous "cycle" (Figure 4A). This surface marks a distinct depositional boundary between the stratified sandstone and the mottled sandstone (Figure 3), whereas the transition from the burrowed sandstone to the overlying mudstone is continuous and gradational, as well as from the mudstone to the stratified sandstone. Therefore, it is much better to define the erosional surface as the base of each cycle. I use the names of W1-W11 to denote cycles defined in this way.

Following this revision, each cycle consists of a transgressive basal sandstone (Facies 1), which fines usually from medium sandstone upward to very fine sandstone, and the overlying progradational coarsening-upward interval (Facies 2–6; Figures 4B and 5). The latter is lithologically subdivided into five sedimentary facies: mudstone (Facies 2), mudstone interbedded with very thin sandstone beds (Facies 3), alternated HCS (hummocky cross-stratification) sandstone and mudstone (Facies 4), amalgamated HCS sandstone (Facies 5), and tabular cross-stratified sandstone (Facies 6; Figure 5). As examples, successions of the cycle W3 and W10 are shown in Figure 5.

Transgressive basal sandstone (Facies 1)

The transgressive basal sandstone (Facies 1) rests on a distinctive erosional surface truncating the upper part of the underlying cycle (Figures 3, 5), and fine upward from medium sandstone to very fine sandstone (Figure 5). This basal sandstone facies is conformably capped with mudstone of the Facies (2) or (3) (Figures 3, 5). The thickness of the basal sandstone attains 5–20 m, and is thin compared with the overlying coarsening-upward interval in each sedimentary cycle (30–100 m).

The basal sandstone is gray to greenish gray in color and includes lithic granules, grains of green smectite, and pum-

➡ **Figure 4.** Lithofacies of the cycles in the Waita Formation. **A.** Erosional basement of the sedimentary Cycle W3, Loc.6005 A shellbed showing a wave dune covers the erosional surface. Hammer is 30 cm long. **B.** Up-coarsening interval (Facies 2–5) in Sedimentary Cycle W5, Loc. 6047. The cliff is 15 m in height. **C.** Vertical profile of the basal sandstone (Facies 1) bioturbated by *Thalassinoides* ichnosp, Loc. 6006. (Natural size.) **D.** Vertical profile of the basal sandstone. Light-colored grains are pumice, dark-colored grains green smectite. Loc. 6098a. (Natural size) **E.** Photomicrograph of top part of basal sandstone (Facies 1), Loc. 6011a. Glauconite grains, gray in the photograph, are abundant. Scale is 0.5 mm long. **F.** *Phycosiphon* ichnosp. in vertical profile of the mudstone with thin sheet sandstone (Facies 3), Loc. 6017. (Natural size.) **G.** *Planolites* ichnosp. in vertical profile of alternation of HCS sandstone and mudstone (Facies 4), Loc. 6102. (Natural size) **H.** Amalgamated HCS sandstone (Facies 5), Loc. 6026. Hammer is 30 cm long.

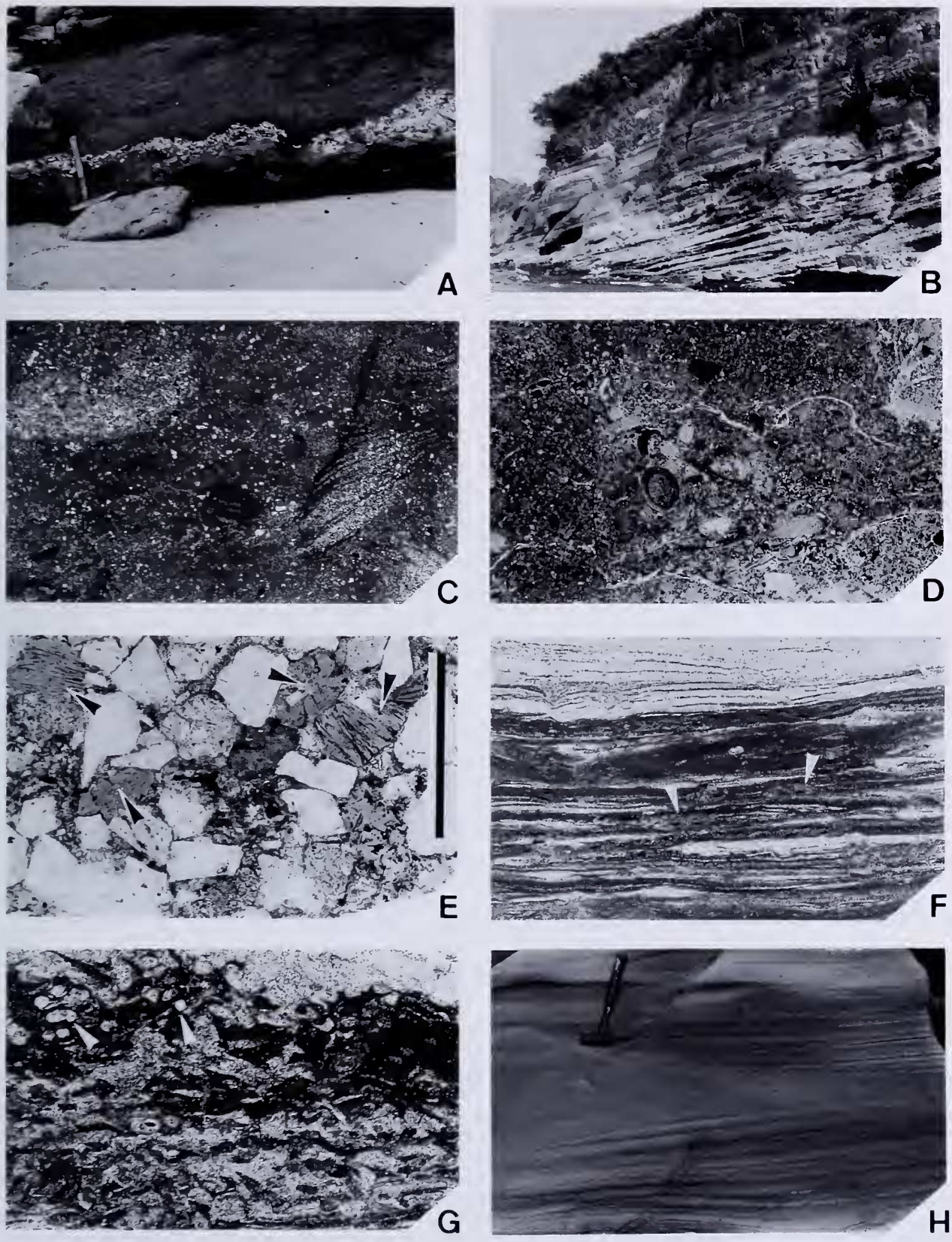
A
B
C
D
E
F
G
H

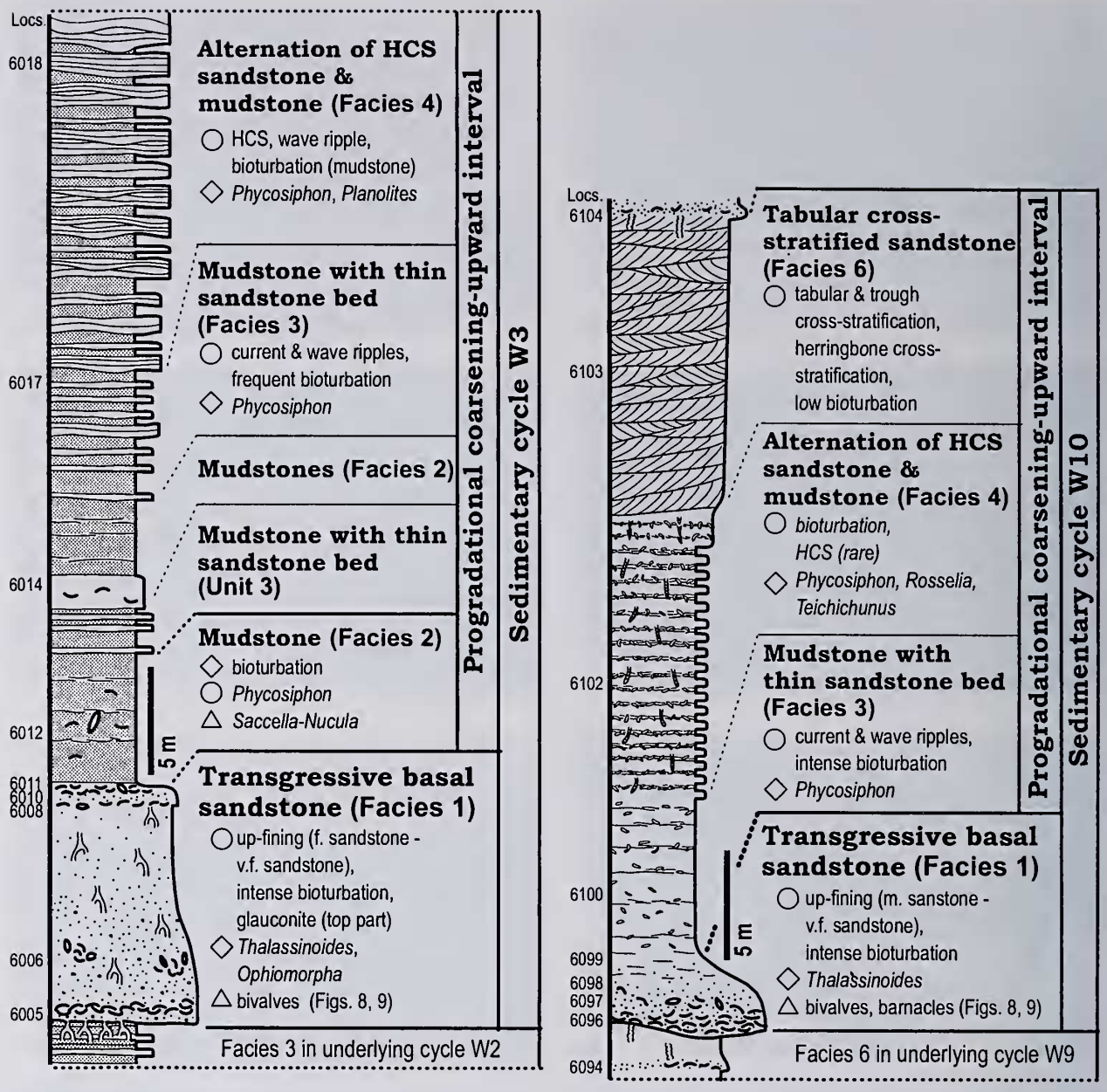

Figure 5. Sedimentary cycles and the lithological facies in the Waita Formation. Each cycle is subdivided into the basal sandstone (Facies 1) and the up-coarsening interval (Facies 2–5 or 6).

➡ **Figure 6.** Modes of fossil occurrence. **A.** Bidirectional imbrications (arrows) of shell fragments of the *Glycymeris-Phacosoma* Assemblage (a) in the basal sandstone (Facies 1) of cycle W3, at Loc. 6005. This sedimentary structure is characteristic of a wave dune.Sscale bar is 2 cm long. **B.** Epifaunal bivalves, *Chlamys* sp. and barnacles of *Venericardia-Crassatella* Assemblage (b2) in the basal sandstone (Facies 1) of cycle W11, at Loc. 6109. Barnacles attach to shell surface. Lens cap is 5.5 cm in diameter. **C.** Matrix of the host sediment of the *Venericardia-Crassatella* Assemblage with abundant epifauna (b2; same as in figure 6B). The shell fragments are concentrated and imbricated in the vertical profile. (X 0.9). **D.** Articulated shells showing geopetal of the *Venericardia-Crassatella* Assemblage (b2; same as in figure 6B). Scale bar is 2 cm long. **E.** Shell replaced by clay minerals of the *Venericardia-Crassatella* Assemblage (b2) in the basal sandstone (Facies 1) of cycle W10, at Loc. 6098a. Scale bar is 1mm long. **F.** Horizontal view of shell clumps (*Venericardia subnipponica*) of the *Venericardia* Assemblage in the middle part of the basal sandstone of cycle W3, at Loc. 4407. Articulated shells are observed. Lens cap is 5.5 cm in diameter. **G.** Profile of the matrix deposits of the *Yoldia-Nucula* Assemblage (d) in the mudstone of the cycle W2, at Loc. 6001a. (Natural size.) **H.** Apices-oriented shells on minor erosional surface of the *Yoldia-Nucula* Assemblage (d; same as in figure 6G). Lens cap is 5.5 cm in diameter. Loc. 6001a.

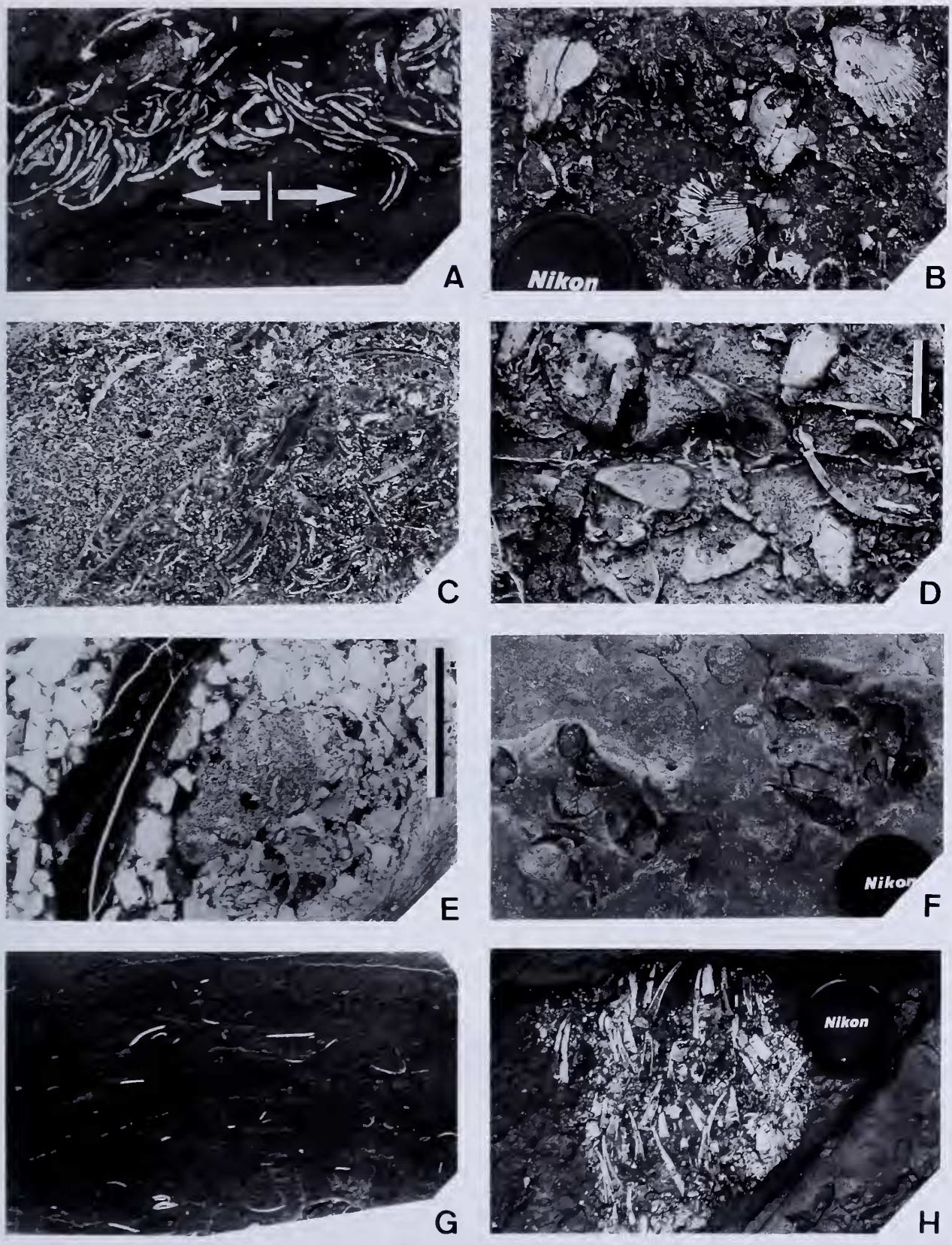
A
B
Nikon
C
D
E
F
Nikon
G
H
Nikon

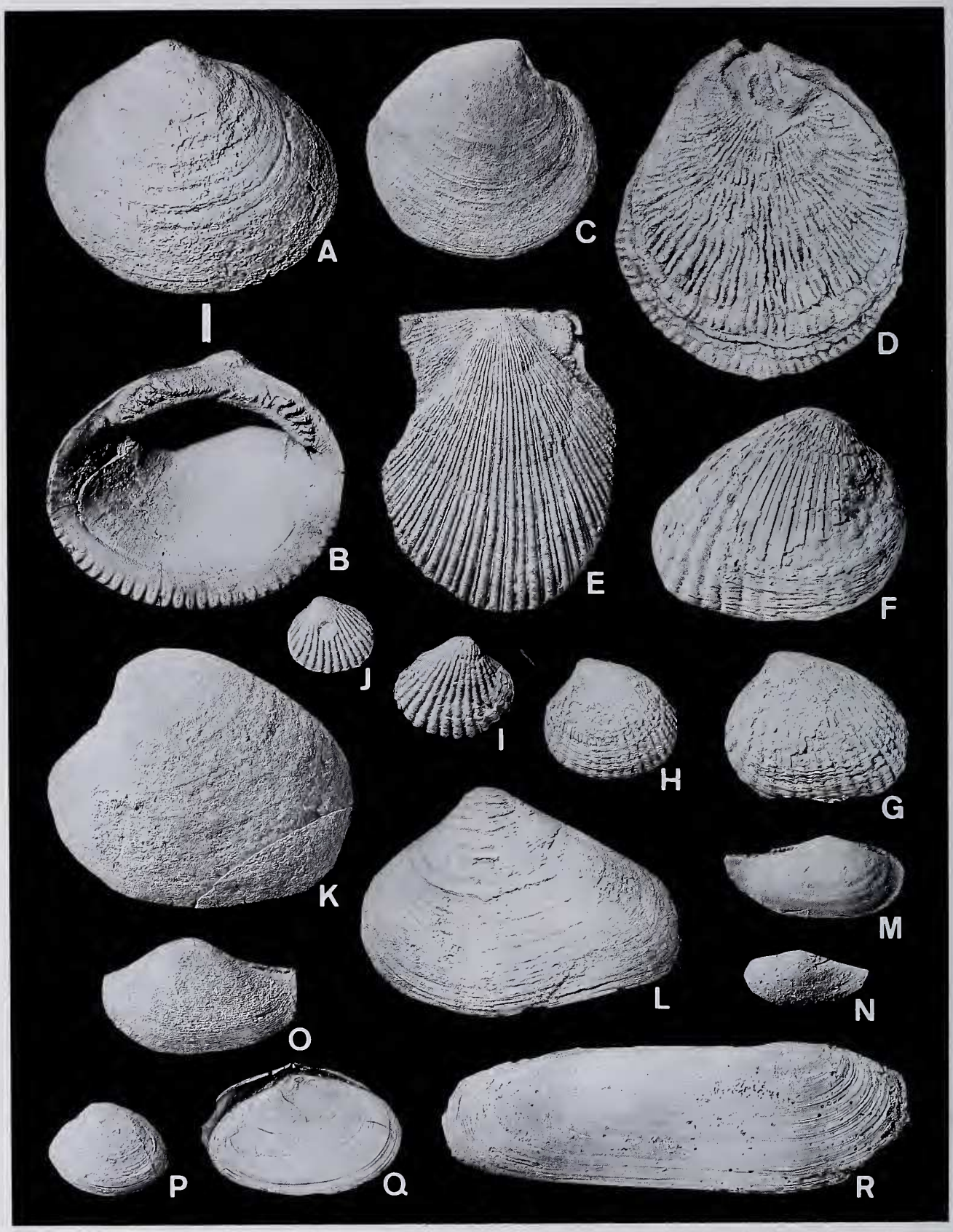
A
C
D
B
E
F
J
I
H
G
K
L
M
N
O
P
Q
R

ice (Locs. 6006, 6082, 6098a; Figure 4D). In cycle W3, many glauconite grains occur, especially from the top part of the transgressive basal sandstone just below the mudstone of Facies (2) (Figures 4E, 5). The basal sandstone is mottled and intensely bioturbated; *Thalassinoides* and *Ophiomorpha* burrows are abundant (Figure 4C). The basal erosional surface is burrowed occasionally by these ichnospecies (Loc. 6005).

In addition to the basal surface, several minor erosional surfaces are recognized, usually within the lower part of the sandstone. These erosional surfaces undulate with relief of up to 30 cm, and are usually overlain by allochthonous shellbeds or pumice layers (Figures 4A, 5). The basal shellbed locally forms small shell mounds on the wavy erosional surface. These shells show bidirectional imbrications (Loc.6005; Figure 6A). Such sedimentary structure characterizes a wave dune (Cheel and Leckie, 1992). Articulated bivalve shells are dispersed as patches in the upper part of the basal sandstone (Figures 5, 6F), in contrast to the allochthonous shellbeds in the lower part of the facies.

Molluscan fossils are abundant (Figure 7). Assemblages of (a) *Glycymeris-Phacosoma*, (b) *Venericardia-Crassatella*, and (c) *Venericardia* occur from this facies (Figure 8; described later).

Progradational coarsening-upward interval (Facies 2–6)

Two types of progradational coarsening-upward intervals are recognized in the Honjo and Waita Formations. The first type is composed of mudstone (Facies 2), mudstone interbedded with very thin sandstone beds (Facies 3), alternated HCS sandstone and mudstone (Facies 4), and amalgamated HCS sandstone (Facies 5) in ascending order. Another type of the coarsening-upward intervals is also composed of the Facies (2–4) capped by tabular cross-stratified sandstone (Facies 6). That is, Facies (6) replaces Facies (5) in the uppermost part of the interval. Facies (5) and (6) do not coexist within a single cycle.

Mudstones (*Facies 2*).—This facies conformably covers the basal sandstone (Facies 1), and characterizes the lowermost part of the progradational coarsening-upward interval (e.g., Cycle W3; Figure 5). It consists of dark gray laminated or bioturbated mudstone 5–40 m thick. Very fine sandstone beds (less than 5 cm thick) are occasionally intercalated in the mudstone (Locs. 4402, 6001a, 6050). *Yoldia-Nucula* Assemblage (Figure 8; described later) and *Phycosiphon* ichnosp. are abundant in the bioturbated parts (Figure 6G).

Mudstone interbedded with very thin sandstone beds (*Facies 3*).—This facies changes transitionally from the underlying mudstone (Facies 2) (Loc. 6012 etc.), or directly covers the basal sandstone (Facies 1) (Locs. 6012 and 6100). It attains 3–10 m thickness (Locs. 4404, 6003, 6052 etc.), and is characterized by mudstone interbedded with very thin sandstone bed of less than 15 cm thickness. The sheet sandstone is very fine, and shows parallel, current and wave ripple laminations.

Primary sedimentary structures are sometimes disturbed by *Phycosiphon* ichnosp. (Figure 4F). The intensely bioturbated part which directly covers the basal sandstone yields various types of ichnofossils (*Planolites*, *Paleophycus*, *Rosselia*, *Skolithos* etc.; Locs. 6088, 6100), and molluscan fossils such as *Acila ashiyaensis* and *Dentalium* sp. etc. (Figure 8).

Alternation of HCS sandstone and mudstone (*Facies 4*).—This facies overlies Facies 3, and is capped with the Facies (5) or (6). It is 3–20 m thick and consists of alternations of sandstone and mudstone (Locs. 6017, 6047, 6101 etc.). The sandstone beds are 15–150 cm thick and tend to thicken upward, and each bed has a slight erosional base. Hummocky cross stratification, parallel lamination and wave ripples are well observed in the sandstone without remarkable signs of bioturbation. In contrast, the interbedded mudstone is commonly bioturbated by *Phycosiphon* ichnosp. (e.g., Cycle W3 at Loc. 6017). In Cycles W9 and W10, both sandstone and mudstone are exceptionally intensely bioturbated by *Phycosiphon* and *Planolites* ichnospp. (Locs. 6089, 6102: Figure 4G), and also yield *Teichichnus* and *Rosselia* ichnospp. *Rosselia* burrows show the upward removal trails to escape from rapid burial (Nara, 1997).

Amalgamated HCS sandstone (*Facies 5*).—This facies consists of amalgamated HCS sandstone, 10 m thick, at the top part of the cycle (Locs. 6026, 6048; Figure 4H). The sandstone is clean, well-sorted and very fine-grained. Primary sedimentary structures, such as hummocky cross-stratification, are well preserved. Mudstone and wave rippled sandstone beds, 20 cm thick, are rarely intercalated in the sandstone. The top of this facies yields many *Ophiomorpha* burrows (Loc. 6027).

Tabular cross-stratified sandstone (*Facies 6*).—Some cycles have tabular cross-stratified sandstone (6) at the top,

← **Figure 7.** Bivalve fossils from the Waita Formation (D, R X0.9; I, M, O, Q X2; N X2.5; J, P X3; others X1). **A, B.** *Glycymeris cisshuensis* Makiyama, Cycle W5 at loc. 6043. **C.** *Phacosoma chikuzenensis* Nagao, Cycle W9 at loc. 6083. **D.** *Monia* sp. Cycle W3 at loc. 6008. **E:** *Chlamys* sp. Cycle W10 at loc. 6098a. **F–J.** *Venericardia subnipponica* Nagao, F, G, H; Cycle W1 at loc. 4309. I, J; Cycle W2 at loc. 6001a. **K.** *Pitar matsumotoi* (Nagao), Cycle W10 at loc. 6083. **L.** *Crassatella yabei* (Nagao), Cycle W5 at loc. 6043. **M, N.** *Yoldia* sp., Cycle W2 at loc. 6001a. **O.** *Saccella* sp., Jinnobaru F. at loc. 3100. **P.** *Nucula* sp., Cycle W2 at loc. 6001a. **Q.** *Angulus maximus* (Nagao), Cycle W2 at loc. 6001a. **R.** *Cultellus izumoensis* (Yokoyama), Jinnobaru F. at loc. 3100. All specimens in this figure are housed in the Kyoto University Museum.

Sedimentary cycle	Locality. no.	Bivalvia																						Gastropoda						others				
		Glycymeris cisshuensis	*Phacosoma chikuzenensis*	*Pitar matsumotoi*	*Meretrix* sp.	*Spisula* sp.	*Crassostrea* sp.	*Crassatella yabei*	*Venericardia subnipponica*	*Chlamys* sp.	*Monia* sp.	*Arca sakamizuensis*	*Clinocardium* sp.	*Felaniella* sp.	*Lucinoma nagaoi*	*Cultellus izumoensis*	*Solamen subfornicatum*	*Periplomya* sp.	*Angulus maximus*	*Saccella* sp.	*Yoldia* sp.	*Acila ashiyaensis*	*Nucula* sp.	"*Diloma*" sp.	*Phyllonoyus ashiyaensis*	*Euspira ashiyaensis*	*Turritella infralirata*	*Turritella karatsuensis*	*Fulgoraria* sp.	*Dentalium* sp.	barnacles	Spatangoida	*Echinodiscus ashiyaensis*	calcareous tube of Serpulid warm
W11	6109	12	5	4				25 (4)	2	27	29													5	2						15		2	2
W10	6098 a		5					33 (6)	37 (12)	31 (2)	8 (4)	2 (2)													4	4			2	2	15			
	6097		14 (2)	16				8	17																									
	6096	58	34					3	7	6																								
W9	6094			5																										6				
	6087																		2 (2)			36 (10)								6				
	6086								53 (8)							14 (8)				42 (2)	4	1	6											
	6083		54	12					26 (4)																						5			
	6082		25 (4)	18 (4)				27	11 (4)																									
W7	6062	10	12	2				8	23																									
W6	6049			5 (2)																														
W5	6043	72	12	2				14																		10								
	6027	6	26	15	1	4																			4									
W4	6022						15																											
W3	6014															10 (8)			10 (4)										12					
	6012															14 (8)			2 (2)		5		8						8					
	6011 a								98 (8)								9 (4)	4 (4)	7	10														
	6010 a		27 (4)	21 (8)				12 (4)	102 (8)	2	3		5	8						5						3								
	6008	3	9 (4)	15 (6)					73 (58)	1	9 (4)															3	6							
	6006								72 (52)																									
	6005	36	33																															
W2	6001 a								4 (2)						4 (2)	23 (22)			16 (10)		35 (8)	1	14			6		4		18				
W3	4407								87 (18)																									
	4406	36	55																															
W2	4402								3							8 (8)			20 (12)		12 (4)	2	8					4		10				
W1b	4217								57 (4)						4 (4)											20			30					
	4315														10											2	34			90					
	4312			1					48 (20)																									
	4310 a								27 (12)						2 (2)	98 (80)										8	50			18	4	1		
	4309								77 (60)							2 (2)				6						2				2				
W1a	4308 a								14 (2)						1						42 (8)													
	4306																				5													

Figure 8. Fossil list in the Waita Formation (route map area). Numbers of articulated bivalve shells is parenthesized.

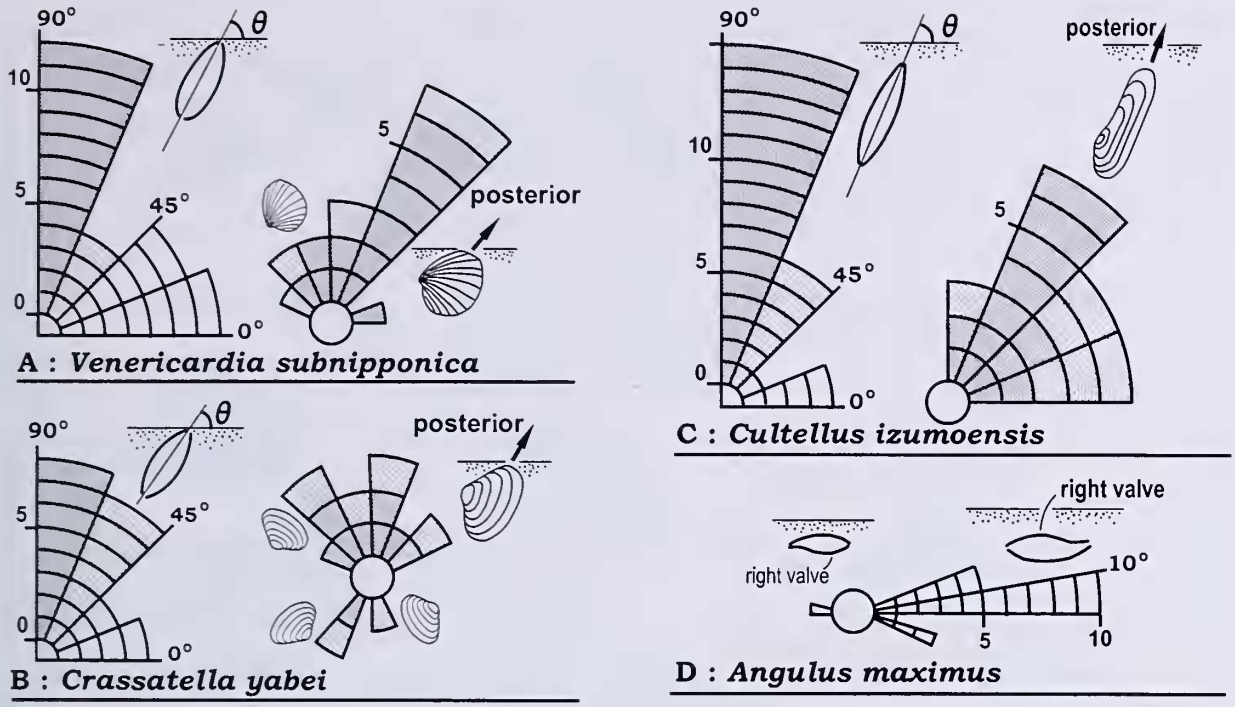

Figure 9. Diagrams showing orientation of articulated bivalve shells in outcrop. **A.** *Venericardia subnipponica* at Loc. 6097, **B.** *Crassatella yabei* at Loc. 6097, **C.** *Cultellus izumoensis* at Loc. 6001a, **D.** *Angulus maximus* (tellinine bivalve) at Loc. 6001a. Left diagrams in A-C show total modes of lateral inclination of commissure planes. Lateral inclinations MORE THAN 45° are stippled by dark or light. Right diagrams in A-C show posteriorwardl direction of selected specimens maintaining their standing positions in the left diagrams (lateral inclinations more than 45° are stippled samples of left diagrams). These articulated shells mainly are elevated in the posterior direction of shell length at angles of about 60°. Darkly or lightly stippled blocks correspond to those areas in left diagrams. D indicates dips of commissure planes and upper valve either left or right. Most articulated *Angulus maximus* lie keeping their right valve up.

instead of Facies (5). Facies (6) consists of tabular and trough cross-stratified fine sandstone 10–15 m thick. Single sets of tabular and trough cross-stratified beds range from 20 to 40 cm thick. Herringbone cross-bedding, tidal-bundle sequences and reactivation surfaces are well observed in the facies (Locs. 6060, 6092, 6102; Sakakura and Masuda, 2001). Lenticular and flaser bedding, 20–30cm thick, is rarely intercalated in the tabular and trough cross-stratified sandstone (Loc. 6070). As in Facies (5), the top of this facies yields many *Ophiomorpha* burrows (Locs. 6094, 6104).

Interpretation of sedimentary environments

Sedimentary environments of transgressive basal sandstone (Facies 1)

The transgressive basal sandstone can be interpreted as the deposits of relative sea level rises during transgression, because signs of wave influence clearly decrease upward. At the base of the basal sandstone (Facies 1), the wave dune is observed on the erosional surface. Such wave dunes strongly suggest deposition under the intense influence of waves in shallow environments (Cheel and Leckie, 1992). No sedimentary structures formed by waves are observed in the upper part of the basal sandstone. Therefore, the upper part of this facies is interpreted to having been deposited below the storm wave base. The view is supported by the fining-upward features of these deposits and the bivalve assemblages whose contents and modes of occurrence differ clearly between the lower and upper parts (discussed later).

Sedimentary environments of coarsening-upward intervals (Facies 2–6)

Progradation of wave-dominated shoreline (Facies 2–5).—The progradational coarsening-upward intervals composed of Facies (2–5) shows wave-influenced sedimentary structures such as wave ripples and hummocky cross-stratification increasing upward.

Facies (2) is the lowermost part of this coarsening-upward interval, and shows no signs of wave-influenced sedimentary structures. It gradually changes upward into

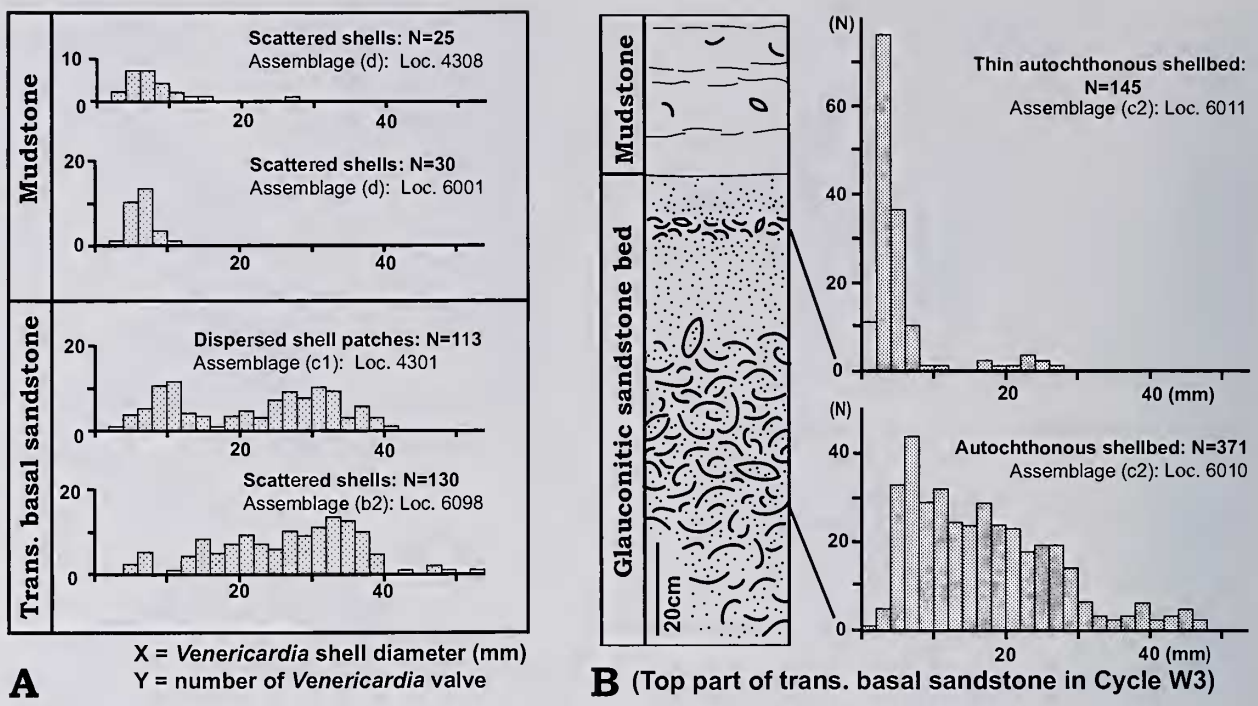

Figure 10. **A**. Size distribution patterns of *Venericardia subnipponica* shells that occur as scattered shells or dispersed shell patches from the basal sandstone (Facies 1) and mudstone (Facies 2). In the basal sandstone, *Venericardia* shells vary in size from less than 10 mm diameter to up to 50 mm. The size-distributional patterns show wide level-curves rather than polymodal ones. In contrast, only small shells, less than 15 mm, occur from the overlying mudstone (Facies 2). **B**. Size-distribution patterns of *V. subnipponica* shells accumulated into autochthonous shellbeds at the top of the basal sandstone. The shell size-distribution pattern in the lower shellbed has a broad range from 2 mm to 48 mm and a gentle and inclined "peak" at 6–8 mm. In contrast, the pattern in the upper shellbed has a very strong mode at 2–4 mm for about 50% of the total number of valves, and with 85% concentrated in the 0–6 mm range.

the overlying Facies (3) in which wave ripple are observable. These features suggest that Facies (2) was deposited below the storm wave base in an outer shelf environment.

Facies(3) and (4) are usually intercalated between the hemipelagic Facies (2) and the amalgamated HCS sandstone (Facies 5). They are characterized by alternation of sandstones that exhibit wave ripples and hummocky cross-stratification, and mudstone. Hummocky cross-stratification is well known in episodic storm deposits (e.g. Dott, Jr. and Bourgeois, 1982). On the other hand, the mudstone represents hemipelagic deposition during fair-weather conditions. Thus, the alternation of sandstones and mudstone (Facies 3 and 4) may suggest deposition above storm wave base and below fair-weather wave base.

The amalgamated HCS sandstone (Facies 5) is the uppermost part of the coarsening-upward interval. This facies is characterized by amalgamated HCS sandstones with few intercalations of hemipelagic mudstone, and indicates deposition above fair-weather wave base. These characters of this facies are typically found in lower shoreface deposits (Walker and Plint, 1992).

The coarsening-upward interval composed of Facies (2–5) may record a successional environmental change from below storm wave base to lower shore face. Such a successional change reflects the progradational processes of a wave-dominated shoreface (*e.g.*, Walker and Plint, 1992).

Progradation of a wave- and tide-influenced shoreline (Facies 2–4 and 6).—Another coarsening-upward interval similarly consists of Facies (2–4) in its lower and middle parts. However, the uppermost part of the interval is replaced by the tabular cross-stratified sandstone (Facies 6), instead of amalgamated HCS sandstone (Facies 5).

The tabular cross-stratified sandstone (Facies 6) overlies inner shelf deposit (Facies 4) and exhibits many tide-influenced sedimentary structures such as herringbone cross-stratification, tidal-bundle sequences, reactivation surfaces, and lenticular and flaser bedding (Nio and Yang, 1989). Based on these features, Facies (6) is interpreted to have accumulated in subtidal or intertidal environments.

The progradational coarsening-upward interval with tidal deposits (Facies 6) at the top also reflects progradational process. In contrast to the coarsening-upward interval of a wave-dominated shoreface, however, it was deposited in a tide- and wave-influenced shelf. Such progradational

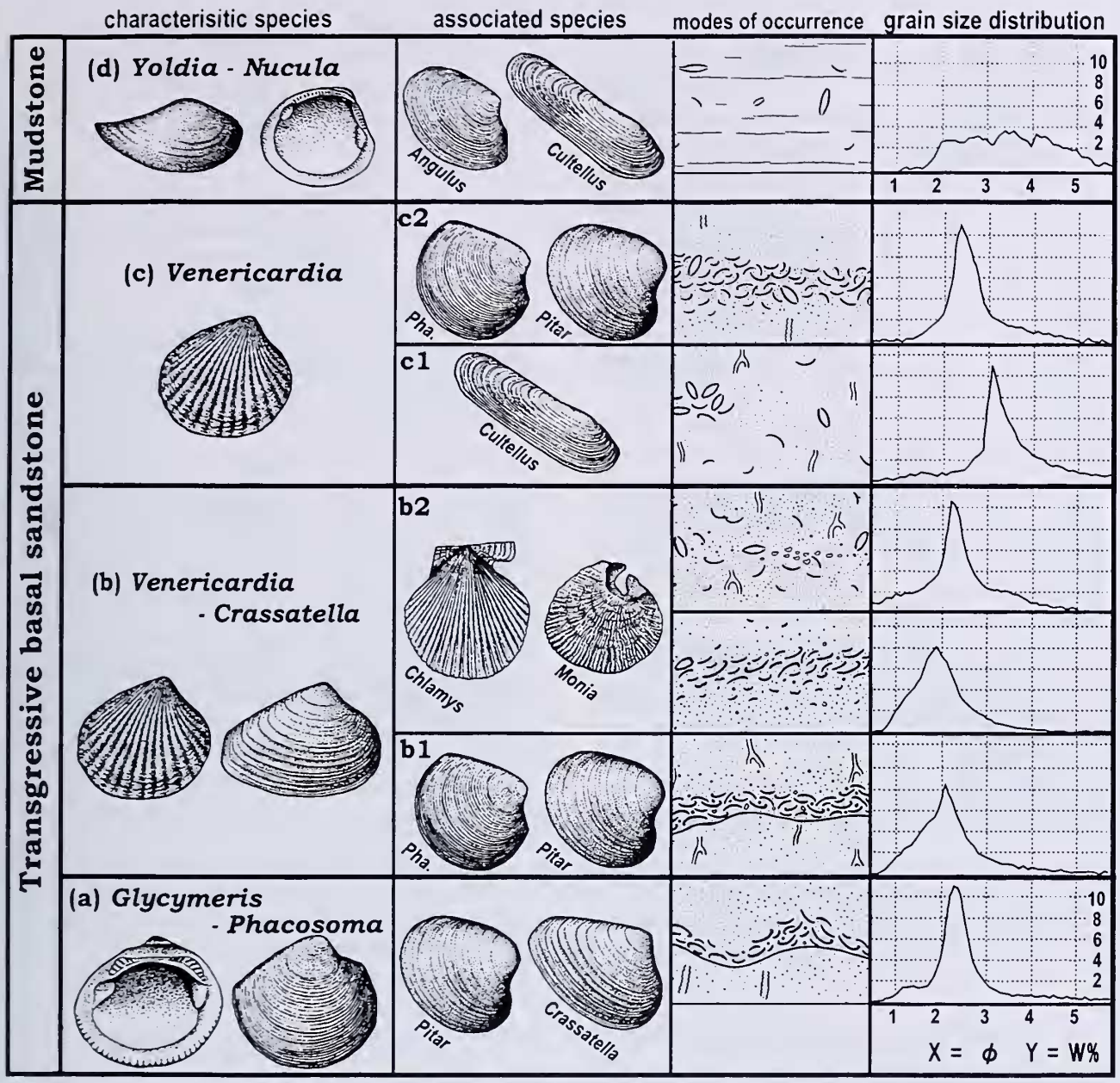

Figure 11. Schematic diagram of bivalve assemblages, showing their compositions, typical modes of occurrence and grain size distributions of the host sediments. The lowermost *Glycymeris-Phacosoma* Assemblage (a) occurs from the well-sorted medium-grained sandstone (Facies 1) as an allochthonous shellbed on the basal erosional surface. On the other hand, the *Yoldia-Nucula* Assemblage (d) indigenously occurs from poorly sorted siltstone (Facies 2). The *Venericardia-Crassatella* and *Venericardia* Assemblages (b, d) show intermediate taphonomic features between the erosional phase and the muddy quiet phase in each cycle.

deposits on a tide- and wave-influenced shelf was reported from the Devonian of the central Appalachian and upper Precambrian of Scotland (Prave *et al.*, 1996; Kessler and Gollop, 1988).

Meaning of redefined sedimentary cycle by sequence stratigraphy

After revision of the cycle boundaries, every cycle can be redefined as a pair of the transgressive basal sandstone that exhibits the decreasing of wave influence, and the progradational coarsening-upward interval of the regressive phase. The new definition seems quite consistent with a

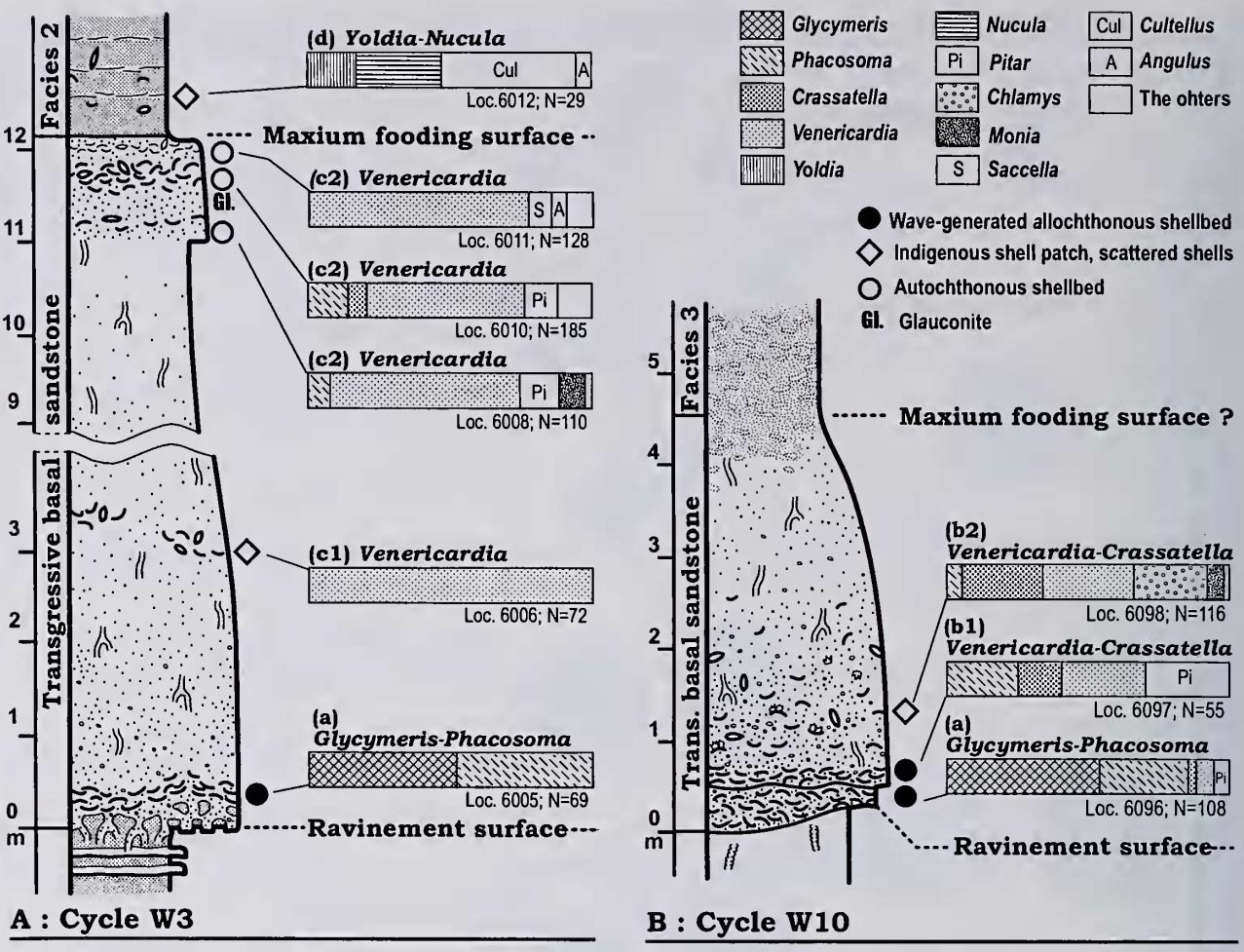

Figure 12. Successive change of fossil bivalve composition in the transgressive basal sandstone (Facies 1) and the lower part of the overlying mudstone (Facies 2). **A.** Cycle W3 and **B.** Cycle W10 are the most typical examples. Four assemblages can be discriminated. *Glycymeris-Phacosoma* Assemblage (a) is replaced upward by the *Yoldia-Nucula* Assemblage (d) via the *Venericardia-Crassatella* (b) and *Venericardia* Assemblages (c). Although all of these assemblages are not always observable in a cycle, the successive change is widespread in every cycle in the Waita Formation.

framework of sequence stratigraphy. The basal sandstone and the coarsening-upward interval reflect the transgressive and high-stand systems tracts, respectively (Posamentier and Vail, 1988). The distinct erosional surface at the base of every cycle probably corresponds with the ravinement surface (transgressive surface; Swift, 1968; Nummedal and Swift 1987), and the glauconitic sandstone beds in the top part of the transgressive basal sandstone in the Cycle W3 (Figure 6E) is regarded probably as the condensed section (Loutit *et al.*, 1988) at maximum flooding surface, which is generated by low sediment supply and slow deposition. Revision of the sedimentary cycles provides a simple but more reasonable paleoenvironmental framework for further studies on paleoecology.

Succession of molluscan assemblages

Molluscan assemblages

Molluscan fossils occur abundantly in, and are stratigraphically restricted to, the transgressive basal sandstone (Facies 1) and the overlying mudstone (Facies 2 and 3) in the lower part of each cycle (Figures 3, 5 and 7). Four different fossil assemblages are distinguished from the viewpoints of faunal composition and modes of occurrence. These four assemblages occur successively within a section, appear repeatedly in every cycle in the same order, and show characteristic taphonomic features. I have examined their modes of occurrence, paying particular attention to articulation and burial position of the shells, shell fabric and fragmentation in shellbeds, articulated bivalve fossils still in life position, and shell size distribution

(Figures 6, 9 and 10). Figure 11 summarizes the contents and modes of occurrence of the four assemblages. The grain size distribution of their host sediments was investigated in detail by a settling tube system. The settling distance was 150 cm, and the cumulative sediment weight was automatically logged by computer.

(*a*) *Glycymeris-Phacosoma Assemblage.*—This assemblage is characterized by *Glycymeris cisshuensis* and *Phacosoma chikuzenensis*, and is associated with *Pitar matsumotoi*, *Crassatella yabei* etc. (Figures 8, 11, 12).

The assemblage (a) characteristically occurs in clean sandstone, which rests directly on the erosional basement (ravinement surface) of the transgressive basal sandstone (Figure 12). The occurrence interval is 50–100 cm thick above the base. The host sandstone is massive or sometimes mottled by bioturbation (Figure 4C, D), and is fine- to medium-grained.

The shells are densely concentrated as an allochthonous shellbed of 20–50 cm thick, on an erosional surface at the base of the cycle (Locs. 6005, 6043, 6096; Figure 4A). The erosional surface shows wavy undulation, whose relief is up to 20 cm high. Bivalve shells are usually disarticulated and somewhat fragmented. They are sometimes piled up and imbricated bidirectionally along both slopes on the crest (Loc. 6005; Figure 6A). These features are characteristic of wave dunes (Cheel and Leckie, 1992).

The assemblage consists mainly of medium- to large-sized shells (30–100 mm). Their calcareous shell tests are occasionally replaced by clay minerals (Figure 6E).

A grain-size distributional pattern of the sandstone matrix is highly concentrated, and the mode lies on fine-grained sand size (ϕ = 2.3 ; Figure 11). Very fine sand or finer grains ($\phi > 3$) do not contribute much (Figure 11).

(*b*) *Venericardia-Crassatella Assemblage.*—The assemblage consists mainly of *Venericardia subnipponica* and *Crassatella yabei* (Figures 11, 12). It is subdivided into two subtypes by differences of the associated species. The first subtype (b1) is associated with *Phacosoma chikuzenensis* and *Pitar matsumotoi* which are common in the *Glycymeris-Phacosoma* Assemblage (a) (Locs. 6082, 6097: Figures 8, 11, 12). The second subtype (b2) is characteristically associated with epibionts represented by epifaunal byssally attached bivalves, *Chlamys* sp. and *Monia* sp., and by barnacles, which attach to molluscan shell surfaces (Locs. 6098a and 6109: Figures 6B, 8, 11, 12).

The first subtype assemblage with *Phacosoma* and *Pitar* (b1) occurs from medium to fine-grained sandstone in the lower to middle parts of the transgressive basal sandstone (Figure 12). The shells occur as allochthonous shellbeds of 20 cm thick on wavy erosional surfaces (Locs. 6082, 6097 etc.), much as those of the *Glycymeris-Phacosoma* Assemblage (a). Green smectite and pumice grains are common in the sandstone. Grain-size distribution of the sandstone matrix shows a moderately concentrated curve (Figure 11). The mode lies on fine-grained sand size (ϕ = 2.2). Silt-size or finer grains, less than 4 ϕ in diameter, do not amount to much.

The second subtype with epifaunal byssally attached bivalves (b2) occurs from medium to fine-grained sandstone 1–2 m thick in the middle part of the basal sandstone (Figure 12). The second subtype assemblage (b2) includes articulated individuals of *Venericardia subnipponica*, *Crassatella yabei* and *Chlamys* sp. (Figures 11, 12). The shells are scattered about the bioturbated sandstone which includes smectite and pumice grains, and which has also little silt or finer grains ($\phi > 4$). The grain-size distributional pattern is similar to that of the first type (b1; Figure 11).

Articulated shells account for 32% of total *V. subnipponica* and 18% of total *C. yabei* shells (Loc. 6098a; Figure 8). Some of them are still in their living position. For example (see Figure 9), twelve among 29 articulated individuals of *V. subnipponica* stand with their commissure plane almost vertical. In this case, most of the standing ones raise their posterior part upward with angles around 60° (Loc. 6098c; Figure 9A). *C. yabei* also exhibits trend similar to that of *V. subnipponica* but the burial pattern is much more dispersed (Loc. 6098c; Figure 9B).

Some disarticulated and articulated bivalve shells are occasionally encrusted by barnacles. Epifaunal byssally attached bivalves such as *Chlamys* sp. and *Monia* sp. are typical examples. They are encrusted not only on the outer side of shells but also on the inner side (encrustation on the inner side indicates that it occurred after the death of the host bivalves). The barnacles keep their attaching colony on the encrusted shell, and the large barnacles shells are consecutively attached by small individuals of new generations. Barnacles also occur as dislocated colonies and disarticulated shell fragments.

The shells of the assemblage (b2) are sometimes accumulated as shellbeds, however, no erosional surface is observed at the base (Loc. 6109). The matrix of the shellbed consists of a mixture of many shell fragments showing imbrications, articulated shells filled by geopetal, and medium- to fine-grained sands (Figure 6C and D). Shell fragments are variously abraded (Figure 6C). Encrustation by barnacles is common on disarticulated bivalve shells (Figure 6B).

In both subtypes (b1 and b2), medium- and large-sized shells of *V. subnipponica* (20–40 mm) are abundant (Locs. 6083, 6095, 6098b). In contrast, small shells less than 10 mm in diameter are few. Figure 10A shows a size-distributional pattern of *V. subnipponica* shells that are scattered about the middle interval of the basal sandstone at Loc 6098b. The smaller-shell portion might have been trimmed off the original thanatocoenosis by fragmentation and winnowing out by wave currents or the replacement of

shell tests by clay minerals (Figure 6E).

(*c*) *Venericardia Assemblage.*—The assemblage is characterized by abundant *Venericardia subnipponica* (Figures 11, 12). The assemblage can be subdivided into two subtypes, c1 and c2, by difference of the associated species (Figure 11). The subtype (c1) consists mostly of *V. subnipponica*, and has very few associated species except for *Cultellus izumoensis* in places (Locs. 4310a, 4313, 6006 etc; Figures 8, 12). The subtype (c2) is characterized by a great quantity of *V. subnipponica*, and associated *Phacosoma chikuzenensis*, *Pitar matsumotoi*, *Monia* sp. and *Crassatella yabei* (Locs. 6009–6011a; Figures 8, 12).

The subtype (c1) occurs commonly from very fine sandstone 8–20 m thick in the middle to upper part of the transgressive basal sandstone (Figure 12). The sandstone yields many *Thalassinoides* burrows (Figure 4C). The *Venericardia* Assemblage (c1) occurs from much more fine-grained deposits than the assemblages (a) and (b). The grain-size distribution curve shifts fineward, and the mode lies on very fine sand size (ϕ = 3). Coarse and medium-grained sands are few.

The subtype (c1) occurs as indigenous shell-patches (Figure 11) or scattered shells. *Venericardia subnipponica* sometimes forms a shell clump composed of tens of articulated individuals (Locs. 4313, 6006; Figure 6F). They frequently keep their living position in bioturbated very fine sandstone. Size distribution pattern of *V. subnipponica* in the subtype (c1) has a wide range (4–40 mm) and polymodal curve (Loc. 4310b; Figure 10A). These features might result from overprinting of indistinguishable populations because of sampling from the thick interval of bioturbated and mottled sandstone.

On the other hand, Subassemblage (c2) is restrictedly found only from a glauconitic sandstone bed at the top of the transgressive basal sandstone in the cycle W3 (successive Locs. 6008, 6010a and 6011a; Figure 12). The shells of the Subtype (c2) accumulated as an autochthonous shellbed (Figures 10B, 11, 12), which contained articulated large *Monia* sp. that probably attached to other shells with a byssus, particularly in their early growth stage (Loc. 6008; Figure 7D). The grain-size distribution curve of the host rock has a mode at very fine sand (ϕ = 2.4; Loc. 6010a; Figure 11), which is slightly coarser than the host rock of the subtype (c1).

A great quantity of disarticulated *V. subnipponica* shells constructs a shellbed 40–60 cm in thickness (Loc. 6010b, Figure 10B). The shellbed starts with a gradual increase of shell content in the lower 20 cm interval, and ends at a sharp top. The shells are oriented at random, and are occasionally attacked by boring polychaetes. The shellbed also yields articulated individuals of *V. subnipponica* and *P. matsumotoi* (Figure 8), some still in their living positions. A quantity of *V. subnipponica* shells has a broad range in shell diameter from less than 2 mm to 48 mm. The histogram of the shell size distribution shows a mode at 6–8 mm for 44 valves of 317; it forms a broad and inclined "peak" that rises swiftly from the smallest shells then declines gradually to the largest ones (Figure 10B lower).

In the transitional zone from glauconitic sandstone to mudstone (Facies 2), the subtype (c2) is composed particularly of many small *V. subnipponica* shells accompanied with *Angulus maximus*, an associated species of the *Yoldia-Nucula* Assemblage (d) at Loc. 6011a (discussed below; Figures 8, 12). Many small *V. subnipponica* shells are concentrated into a thin shellbed 2–5 cm in thickness. The histogram of the shell diameter distribution shows a high mode at the 2–4 mm; range, in which about 50% of the total of 145 valves are included. More than 85% of the valves fall in the range of 0–6 mm, and otherwise medium-sized shells (10–30 mm) account for only about 7% (Loc. 6011b; Figure 10B). A similar distributional tendency of *V. subnipponica* shell diameters is represented in the *Yoldia -Nucula* Assemblage (d) (described immediately below).

(*d*) *Yoldia-Nucula Assemblage.*—The assemblage consists mainly of *Yoldia* sp., *Nucula* sp., *Angulus maximus*, *Cultellus izumoensis*, *Venericardia subnipponica*, *Dentalium* sp. (Locs. 6001a and 6012; Figures 8, 11, 12). Unlike the other assemblages, the *Yoldia-Nucula* assemblage occurs from the bioturbated mudstone (Facies 2; Figure 6G) which overlays the basal sandstone (Facies 1) at Locs. 4308a and 6012 (Figure 10), and the grain size distributional pattern shows a broad curve extending from fine sand size (ϕ = 2) to silt size (ϕ = 5; Figure 11) without an obvious peak.

Usually, the molluscan fossils are scattered about the mudstone (Figure 6G). Some bivalve shells of *Yoldia* sp. and *Nucula* sp. are articulated and arranged at random. Most *Cultellus izumoensis* shells are articulated (Loc. 6001a; Fgiure 8). Among 26 articulated individuals, fifteen *C. izumoensis* stand with their commissure plane subvertical, and frequently the posterior part is raised upward at angles around 60° (Loc. 6001c; Figure 9C). The shells of *Angulus maximus* (= tellinine bivalve) are also articulated in high numbers (Loc. 6001a; Figure 8), and retain their living position, in which their right-warped siphonal gape is oriented upward. Their articulated shells lie horizontally in the matrix still keeping their right valve uppermost. (Loc. 6001c; Figure 9D).

Shells of *Dentalium* sp. and *Turritella karatsuensis* occur occasionally as allochthonous shell stringers (Kidwell *et al.*, 1986) on minor erosional surfaces (Loc. 6001a). The horn- or drill-shaped shells are concentrated in parallel and arranged into a scar 50 cm long and 20 cm wide, and their apices are unimodally pointed (Figure 6H).

Venericardia subnipponica occurs not only from the basal sandstone (Facies 1) but also from the mudstone

(Facies 2). In the *Yoldia-Nucula* Assemblage (d), *V. subnipponica* is a subordinate species, and is represented only by small individuals. It accounts only for 4.1% of in total 97 individuals in the assemblage (b) at Loc. 6001a (Figure 8). Figure 10A show two shell diameter distributional histograms at localities 6001b and 4308b. The pattern at Loc. 6001b has a mode at 6–8 mm, and shells larger than 12 mm diameter are scarce.

Successive occurrences of molluscan assemblages

The molluscan assemblages change successively in upward sequence within the transgressive basal sandstone and the overlying mudstone in each cycle. The successive occurrences are similarly made up of, in ascending order, the (a) *Glycymeris-Phacosoma* Assemblage, (b) *Venericardia-Crassatella* Assemblage, (c) *Venericardia* Assemblage and (d) *Yoldia-Nucula* Assemblage (Figure 11). Their successive occurrence is never reversed in order, and is uniformly repeated in every sedimentary cycle, though all the four assemblages are not always completely observable within a cycle. Related to the faunal change, their typical modes of occurrence shift upward from allochthonous shellbed into indigenous shell clumps and patches.

The most typical examples of the Cycles W3 and W10 are summarized in Figure 12. In cycle W3 (Locs. 6005–6012; Figure 12A), the faunal succession starts with the *Glycymeris-Phacosoma* Assemblage (a), which occurs only as the basal allochthonous shellbed with wave dunes at the base of the cycle (Locs.6005). The *Venericardia-Crassatella* Assemblage (b) is skipped there. The lowermost assemblage (a) is replaced upward directly by the *Venericardia* Assemblage (c) at the 3 m-level above the base. The top part of the occurrence range of the assemblage (c) intercalates with *V. subnipponica* shellbeds in glauconitic sandstone bed that indicates the surface of maximum transgression (11–12 m level in figure 12A). The shellbeds also yield a few *Phacosoma chikuzenensis* and *Pitar matsumotoi*, both of which are associate species of the Subassemblage (c2). The indigenous *Yoldia-Nucula* Assemblage (d) appears at the 12.5 m-level as the lithology changes quickly from sandstone to the overlying mudstone (Facies 2).

The faunal succession is almost identical in the Cycle W10, but is condensed within a thin basal interval (0–2 m level in Figure 12B). The *Glycymeris-Phacosoma* Assemblage (a) is also dominant on the basal erosional surface, and is similarly replaced upward by the *Venericardia -Crassatella* Assemblage (b1) on the erosional surface at the level of 0.5 m above the base (Loc.6096–6097; Figure 12B). The latter assemblage (b1) is immediately succeeded by another subtype (b2) of the *Venericardia-Crassatella* Assemblage with abundant epibionts, such as *Chlamys* sp., *Monia* sp. and barnacles, at the level of 0.7 m above the base (Loc. 6097, 6098a: Figure 12B). The occurrence range of Assemblage (b2) encompasses 1.5 m in thickness, and is terminated with an increase of mud content in the host rock (Figure 12B).

Discussion

Taphonomic implication of faunal change in cycles

Molluscan fossils mostly occur from the lower part of each cycle, i.e., the transgressive basal sandstone (Facies 1) and the mudstone (Facies 2) that had been deposited during the earliest regressive phase (Figure 12). Four distinctive fossil assemblages are preserved in this relatively thin part. Close taphonomical observation can "decode" the hidden paleoenvironmental and paleoecological changes condensed in this transgressive interval in high resolution.

The lowermost *Glycymeris-Phacosoma* Assemblage (a) occurs only as allochthonous shellbeds on the erosional base of the transgressive basal sandstone (Figures 11, 12). Most of the shells are disarticulated completely and fragmented considerably there, and often form wave dunes (Cheel and Leckie, 1992: Figure 6A). The matrix of the host rock is well-sorted, fine-grained sandstone, and the mud content is small (Figure 11). These features strongly suggest deposition under intensely wave-influenced conditions, in which the sea bottom is frequently eroded and shells are easily winnowed. The molluscan shells in this assemblage might be reworked repeatedly even if they were not transported horizontally far from their habitats. The succeeding *Venericardia-Crassatella* Assemblage associated with *Phacosoma* and *Pitar* (b1) occurs also as wave-influenced shellbeds on additional minor erosional surfaces (Figure 11)

In contrast, no signs of bottom erosion and shell reworking by wave currents are observable in the upper part of Facies (1) and, also in Facies (2). The *Venericardia* Assemblage (c) consists partly of autochthonous or indigenous shell patches. in the upper part of the basal sandstone (Facies 1), whose grain size distributional pattern shifts fineward ($\phi > 3$: Figure 11).

The uppermost *Yoldia-Nucula* Assemblage (d) occurs mostly as indigenous scattered shells in the overlying mudstone (Facies 2; Figure 12). Their shells are often articulated and found in their living positions (Figure 10). These are no signs of bottom erosion and shell reworking. The host rock contains very fine sand ($2 < \phi < 3$) but is dominated by muds (Figure 11). Allochthonous shells of *Dentalium* sp. and *Turritella karatsuensis* are sometimes accumulated in depressions on the bedding plane of the mudstone, and show preferred orientation (Facies 2; Figure 6H). The cause of such apex-oriented shell stringers is not attributable to waves but to unidirectional currents (Nagle, 1967; Figure 6H).

The successional change of these taphonomic features suggests that the faunal succession is closely associated with the upward decreasing of wave influence. The *Glycymeris-Phacosoma* Assemblage (a) is replaced upward by the *Yoldia-Nucula* Assemblage (d) via the *Venericardia-Crassatella* and *Venericardia* Assemblages (b, c), while the strong wave influence declines from the erosional and winnowing phase to the quiet muddy phase through the transgression period.

Successive faunal change within a sedimentary cycle is widespread and exhibited repeatedly in the Waita Formation. The *Glycymeris-Phacosoma* Assemblage always occurs as the allochthonous shellbed, which corresponds to an onlap shellbed (Kidwell, 1991) on the ravinement surface that indicates early transgression. The other assemblages also retain the autochthonous or indigenous occurrences above this onlap shellbed. Besides the Ashiya Group, similar faunal change in and above onlap shellbeds is observable in the other Paleogene deposits (e.g., the Nishisonogi Group and Hioki Group). Therefore, it seems one of the basic sedimentological and paleoecological features of the Paleogene deposits in west Japan.

Epibionts-enriched fauna

The successive faunal records are sometimes condensed within a very short interval in a cycle, for example, within an interval of 2 m thick from the base in the cycle W10 (Figure 12). Intermittent and limited deposition of this interval is suggested by abundant occurrence of epibionts. Epifaunal byssally attached bivalves: *Chlamys* sp. and *Monia* sp., and barnacles occur commonly as associated species of the *Venericardia-Crassatella* Assemblage (b) from the lower middle part of the transgressive basal sandstone (Figure 12). Some of them are found in the attaching position *in situ* (Figure 6B), while others are fragmented, abraded, and finally assimilated into the shellbed matrices showing imbrications (Figure 6C). Scarcity of fine-grained sediments in the matrix also implies that this component was winnowed out and swept away by currents (Subassemblage b2; Figure 11).

These epifaunal byssally attached bivalves and barnacles require the peculiar condition that their attachment to shelly ground avoids burial by the winnowing out of sediments. A number of shells have been attached by plural generations of barnacles (Loc. 6098a). Some other shells have repeatedly settled by epibionts after death. *Chlamys* and *Monia* probably attached to other shells by their byssus at least in the early ontogenetic stage, although the attachment position is not observable in the fossil record since the byssus is missing. The line of evidence converges to an argument that the shelly ground, which lifts the restriction on the migration of the epibionts, was exposed for a long time. The signs of taphonomic feedback , by which the skeletal remains of dead organisms impact on the next living community (Kidwell and Jablonski 1983), are observable in places (Locs. 6008, 6098a and 6109). The epifaunal byssally attached bivalves cannot survive on the seafloor in which sediments are rapidly and continuously deposited; the same is true of the cemented barnacles, because they have neither a foot to escape rapid burial nor a siphon (Stanley, 1970; Kranz, 1974). The epibiont-rich shellbeds at least in three cycles might indicate strong or gentle current-influenced conditions in which sedimentation was intermittent, and probably, relatively slow.

Autochthonous shellbed in glauconitic sandstone

The glauconitic sandstone bed at the top of the transgressive basal sandstone intercalates with autochthonous shellbeds composed of a great quantity of *Venericardia subnipponica* shells (Subassemblage c2; Locs. 6010 and 6011). Unlike the allochthonous shellbed on the ravinement surface at the base of the cycle, the shellbed at the top is autochthonous because bivalve fossils often keep their living position (Figures 10B, 12). Abundant glauconite grains in matrices (Figure 4E), which develop in areas characterized by low sedimentation (Chamley, 1989), imply condensation as a process of shell accumulation *in situ* during a relatively long period. This view is also supported by the occurrence of epifaunal byssally attached bivalves such as *Monia* sp.

The shell diameter distributional pattern of *V. subnipponica* in this shellbed is shown in Figure 10B (lower). These shells range in length from 2 to 48 mm, with a low mode at 6–8 mm. This may suggest a continuous and stable supply of dead shells of all growth stages *in situ*, which consist of many juveniles and a few mature specimens, except for very small juveniles that have little fossilization potential. As noted above in the sequence stratigraphic interpretation of the sedimentary cycle, the glauconitic sandstone where the autochthonous shellbed lies is regarded as a condensed section associated with the maximum-flooding surface (Figures 5, 12B).

The autochthonous shellbed in the glauconitic sandstone probably reflects attrition from a normal population or "cemetery" (Ager, 1963; Dodd and Stanton, Jr., 1990). It is produced by repetitive colonization of *Venericardia subnipponica* populations *in situ* under low sedimentation rate during the maximum-flooding period. Such a shellbed at the top of a transgressive deposit is classified as a backlap shellbed by Kidwell (1991).

On the other hand, another autochthonous shellbed is intercalated in the transitional zone from the glauconitic sandstone to overlying mudstone (Facies 2) (Figure 10B, upper).

It is composed mostly of small shells of *Venericardia*

subnipponica, some of which are articulated (Figure 10B). In contrast to the *Venericardia* Assemblage in the glauconitic sandstone, the size-distributional pattern of the present species shifts strongly to the smallest portion (Figure 10B upper). The mode of the histogram lies at 2–4 mm, in which more than 50% of the total individuals are concentrated. These features probably suggest that a mass mortality of juvenile shells occurred after an opportunistic larval settlement, and that these shells represent a census population (Ager, 1963; Dot and Stanton Jr., 1990).

Venericardia is a typical infaunal nonsiphonate suspension feeder having limited mantle fusion. They are usually shallow and slow burrowers (Stanley, 1970), and have low escape ability from rapid burial (Kranz, 1974). Consequently, the mass mortality may be involved with the incidental deposition of soupy muds that caused an obrution. The population of *Venericardia* juveniles might be smothered by the obrution event in the transitional phase between condensed glauconitic and muddy. It should be noted that *Venericardia* populations in the overlying mudstone (Facies 2; *Yoldia-Nucula* Assemblage) are also restricted to small-diameter shells.

Conclusion

Based on detailed observations, 11 sedimentary cycles in the upper part of the Ashiya Group (upper Oligocene) were revised and redefined here (Figure 5). Each cycle consists of a basal erosional surface overlain by a transgressive basal sandstone and a progradational-interval of mudstones and sandstones. In this revision, every cycle is bordered by an erosional surface at the base of a fossiliferous sandstone. Four molluscan fossil assemblages are distinguished. They exhibit similar successive occurrences accompanied with transitions of sedimentological and taphonomical features. These are a key to understanding the Paleogene stratigraphy and paleoecology, because similar successive occurrences of bivalve fossils are widespread in other Paleogene deposits in western Japan (i.e., Nishisonogi and Hioki Groups). The successive occurrence of bivalve fossil faunas is interpreted to result from transgressive-regressive shifts in sedimentary regimes (variable wave influence and sediment supply).

Paleoecological aspects of Paleogene bivalves, for example *Venericardia*, still remain obscure. Unlike Neogene or Quaternary fauna, direct analogies from the ecology of modern relatives should not be simply drawn for Paleogene bivalves. On the other hand, taphonomic and sedimentologic aspects can be directly read from the strata. Sedimentary regime seems to be a factor in defining the habitats of bivalves, and is regarded as the most important environmental factor controlling morphologic adaptations of bivalves (Stanley, 1970), owning to their benthic habitat, which not only is closely related to the depositional substrate, but also contains many infaunal styles of burrowing into deposits. Therefore, taphonomic and sedimentologic observation will be a key to understanding the paleoecology of Paleogene bivalve fauna.

Acknowledgments

I would like to express my gratitude to H. Maeda (Kyoto University) for his critical reviews and kind guidance of the manuscript. I am deeply indebted to F. Masuda and T. Sakai (Kyoto University) for their sedimentological cooperation in the field and laboratory, and to Y. Kondo (Kochi University) for his helpful suggestions and encouragements. I am also grateful to S. M. Kidwell (University of Chicago) and an anonymous referee for their helpful comments to improve the manuscript. Thanks are also extended to T. Komatsu (Kumamoto University) and B. Tojo (Kyoto University) for their valuable comments, and staff of Tsuyazaki Fishery Research Laboratory of Kyushu University for their help during fieldwork. This study has been partly supported by a grant-in-aid from the Fukada Geological Institute.

References

Ager, D. V., 1963: *Principles of Paleoecology*, 371 p. McGraw-Hill Co., New York.

Cheel, R. J. and Leckie, D. A., 1992: Coarse-grained storm beds of the Upper Cretaceous Chungo Member (Wapiabi Formation), southern Alberta, Canada. *Journal of Sedimentary Petrology*, vol. 62, no. 6, p. 933–945.

Chamley, H., 1989: *Clay Sedimentology*, 623 p. Springer-Verlag Berlin.

Dott, J. R. and Stanton, Jr., R. J., 1990: *Paleoecology, Second Edition*, 502 p. A Wiley-Interscience Publication John Wiley and Sons, New York.

Dott, Jr., R. H. and Bourgeois, J., 1982: Hummocky stratification: Significance of its variable bedding sequences. *Geological Society of America Bulletin*, vol. 93, p. 663–680.

Hayasaka, R., 1991: Sedimentary facies and environments of the Oligocene Ashiya Group in the Kitakyushu-Ashiya area, Southwest Japan. *The Journal of Geological Society of Japan*, vol. 97, p. 607–619. *(in Japanese with English abstract)*

Loutit, T.S., Hardenbol, J., and Vail, P.R., 1988: Condensed sections: the key to age determination and correlation of continental margin sequences. *In*, Wilgus, C. K. *et al. eds., Sea-level Changes—an Integrated Approach*, SEPM, Special Publication, no. 42, p. 183–213.

Kessler, L.G. and Gollop, Ian.G., 1988: Inner shelf/shoreface-intertidal transition, Upper Precambrian, Port Askaig Tillite, of Islay, Argyll, Scotland. *In*, de Boer, P.L., van Gelder, A. and Nio, S.D. *eds., Tide-influenced Sedimentary Environments and Facies*, p. 341–358. D. Reidel Publishing Company, Boston.

Kidwell, S. M., 1991: Condensed deposits in siliciclastic sequences: expected and observed features. *In*, Einsele, G., Ricken, W. and Seilacher, A. *eds., Cycles and Events in Stratigraphy*, p. 182–195. Springer-Verlag, Berlin Heidelberg.

Kidwell, S. M. and Jablonski, D., 1983: Taphonomic feedback: ecological consequences of shell accumulation. *In*, Tevesz, M. J. S. and McCall, P. L. *eds.*, *Biotic Interaction in Recent and Fossil Benthic Communities* (*Topics in Geobiology 3*), p. 195–248. Plenum Press, New York.

Kidwell, S. M., Fürsich, F. T. and Aigner, T., 1986: Conceptual framework for the analysis and classification of fossil concentrations. *Palaios*, vol. 1, p. 228–238.

Kranz, P. M., 1974: The anastrophic burial of bivalves and its paleoecological significance. *Journal of Geology*, vol. 82, p. 237–265.

Mizuno, A., 1963: Paleogene and Lower Neogene biochronology of West Japan (III. Stratigraphic and geographic distributions of molluscan faunas in West Japan). *The Journal of Geological Society of Japan*, vol. 69, p. 38–49. (*in Japanese with English abstract*)

Nagao, T., 1927a: The Palaeogene stratigraphy of Kyushu (Part 17). *Journal of Geography*, vol. 39, p. 665–674. (*in Japanese*)

Nagao, T., 1927b: Palaeogene fossils of the Island of Kyushu, Japan, Part 1. *Science Reports of Tohoku Imperial University*, vol. 9, no. 3, p. 97–128.

Nagao, T., 1928a: The Palaeogene stratigraphy of Kyushu (Part 20). *Journal of Geography*, vol. 40, p. 143–155. (*in Japanese*)

Nagao, T., 1928b: Palaeogene fossils of the Island of Kyushu, Japan, Part 2. *Science Reports of Tohoku Imperial University*, vol. 12, no. 1, p. 1–140.

Nagle, J. S., 1967: Wave and current orientation of shells. *Journal of Sedimentary Petrology*, vol. 37, no. 4, p. 1124–1138.

Nara, M., 1997: High-resolution analytical method for event sedimentation using *Rosselia socialis*. *Palaios*, vol. 12, p. 489–494.

Nio, S. D. and Yang, C. S., 1989: Diagnostic criteria for recognized tidal dominance in shallow marine clastic deposits. *Short Course Note Series #61*, p. 25–75. International Geoservices BV, Leiderdorp.

Nummedal, D. and Swift, D. J. P., 1987: Transgressive stratigraphy at sequence-bounding unconformities: some principles derived from Holocene and Cretaceous examples. *In*, Nummedal, D., Pilkey, O. H. and Howard, J. D. *eds.*, *Sea-level Fluctuation and Coastal Evolution. SEPM, Special Publication*, no. 41, p. 241–259.

Okabe, M. and Ohara, J., 1972: Variation of heavy mineral assemblage from the Otsuji Group to the Ashiya Group, Chikuho Coal-field, northern Kyushu. *Reports of Earth Science College of General Education, Kyushu University*, vol. 17, p. 59–71.

Otsuka, Y., 1939: Tertiary crustal deformation in Japan—with short remarks on Tertiary paleogeography. *Jubilee Publication in the Commemoration of Professor H. Yabe, M. I. A., 60th Birthday*, vol. 1, p. 481–519. Yabe Kyoju Kanreki Kinen Kai, Sendai.

Oyama, K., Mizuno, A. and Sakamoto, T., 1960: *Illustrated Handbook of Japanese Paleogene Molluscs*, 224 p. Geological Survey of Japan.

Ozaki, M., Hamada, S. and Yoshii, M., 1993: *Geology of the Orio District. with Geological Sheet Map at I: 50,000*, 121 p. Geological Survey ofJapan. (*in Japanese with English abstract*)

Posamentier, H. W. and Vail, P. R., 1988: Eustatic controls on clastic deposition II—Sequence and systems tract models. *In*, Wilgus, C. K. *et al. eds.*, *Sea-level Changes—an Integrated Approach, SEPM, Special Publication*, no. 42, p. 183–213.

Prave, A. R., Duke, W. L. and Slattery, W., 1996: A depositional model for storm- and tide-influenced prograding siliciclastic shorelines from the Middle Devonian of the central Appalachian foreland basin, USA. *Sedimentology*, vol. 43, p. 611–629.

Sakakura, N. and Masuda, F., 2001: Macro-tidal deposits showing semi-diurnal with a diurnal inequality of low water in Paleogene Kyusyu, Japan. *In*, Park, Y. A. and Davis, R. A., Jr. *eds.*, *Proceedings of Tidalites 2000*, p. 87–96. The Korean Society of Oceanography, Special Publication, Seul.

Saito, T. and Okada, H., 1984: Oligocene calcareous plankton microbiostratigraphy of the Ashiya Group, North Kyushu: *In*, Saito, T., Okada, H. and Kaiho, K. *eds.*, *Biostratigraphy and International Correlation of the Paleogene System in Japan*, p. 85–87. Faculty of Science, Yamagata University,

Shuto, T. and Shiraishi, N., 1971: A note on the community-paleoecology of the Ashiya Group. *Science Reports of Faculty of Science, Kyushu University, Ser. D, Geology*, vol. 10, no. 3, p. 253–270.

Stanley, S.M., 1970: Relation of shell form to life habit in the Bivalvia (Mollusca). *Geological Society of America, Memoir 125*, p. 1–296.

Swift, D. J. P., 1968: Coastal erosion and transgressive stratigraphy. *Journal of Geology*, vol. 76, p. 444–456.

Tsuchi, R., Shuto, T. and Ibaraki, M., 1987: Geologic ages of the Ashiya Group, North Kyushu from a viewpoint of planktonic foraminimera. *Reports of Faculty of Science, Shizuoka University*, vol. 21, p. 109–119.

Walker, R. G. and Plint, A. G., 1992: Wave and storm dominated shallow marine systems. *In*, Walker, R. G. and James, N. P. *eds.*, *Facies Models: Response to Sea Level Change*, p. 219–238. Geological Association of Canada, St. John's, Newfoundland.